Coordination Chemistry Reviews, 97 (1990) 1–22
Elsevier Science Publishers B.V., Amsterdam — Printed in The Netherlands

THERMAL AND LIGHT-INDUCED SPIN CROSSOVER IN IRON(II) COMPLEXES

Philipp Gütlich and Andreas Hauser
Institut für Anorganische Chemie und Analytische Chemie
Johannes Gutenberg Universität, D-6500 Mainz, FRG

ABSTRACT - Recently, we have discovered a fascinating photophysical effect in spin crossover complexes of iron(II) : Light-Induced Excited Spin State Trapping (LIESST). At sufficiently low temperatures, the low spin state ($^1A_1$) can be converted quantitatively to the high spin state ($^5T_2$) by irradiating the sample into the $^1A_1 \rightarrow {}^1T_1$ d-d absorption band (~ 540 nm). The resulting metastable HS state has a very long lifetime at low temperatures, in some cases it does not decay noticeably over a period of several days at 10 K. Only at temperatures above some critical temperature does thermal relaxation back to the LS state set in. The sample can also be reconverted to the LS state by irradiating into the $^5T_2 \rightarrow {}^5E$ absorption band (~850 nm). The system thus behaves like an optical switch. The relative positioning - horizontally and vertically - of the potential wells of the two spin states is crucial for the lifetime of the metastable HS state.

1. INTRODUCTION

It is well known that certain octahedral transition metal complexes with four to seven d-electrons can change their spin state from low spin (LS) at low temperatures to high spin (HS) at elevated temperatures. This phenomenon has been termed "spin crossover" or, equivalently, "temperature dependent spin transition".

The first examples of spin crossover compounds were found more than fifty years ago, when Cambi et al. (ref. 1) reported on drastic changes of the magnetic susceptibility in tris(N,N-dialkyldithiocarbamato)iron(III) complexes on varying the temperature. More than thirty years later Baker et al. (ref. 2) found the first iron(II) complex exhibiting a temperature dependent spin transition, viz. $[Fe(phen)_2\ (NCS)_2]$ (phen = phenantroline). In the meantime a large number of spin crossover compounds have been added to this list by various research groups, primarily complexes of iron(II), iron(III), and cobalt(II). The field of temperature dependent spin crossover has been extensively reviewed by many authors (refs. 3-7).

0010-8545/90/$07.70 © 1990 Elsevier Science Publishers B.V.

In the course of our investigations of spin crossover in crystalline iron(II) complexes we accidentally discovered a new effect in 1984 : In the spin crossover system $[Fe(ptz)_6](BF_4)_2$ (ptz = 1-propyltetrazole), which shows a thermal spin transition $^1A_1$ (LS) $\rightleftarrows$ $^5T_2$ (HS) (notation in O_h symmetry) at ~ 130 K, a LS → HS spin state conversion can also be achieved at 10 K by irradiating the crystals with green light (refs. 8,9). Surprisingly, the metastable HS state shows extremely long lifetimes, on the order of days, below ~ 50 K. We have called this unusual photophysical effect "Light-Induced Excited Spin State Trapping (LIESST)". Somewhat later we demonstrated that the reverse process ("Reverse LIESST") is also possible, viz. a light induced HS → LS conversion at 10 K using red light (ref. 10).

Meanwhile, we have observed LIESST and Reverse-LIESST in a number of iron(II) spin crossover systems, although the critical temperature for the thermal back relaxation to the thermodynamically stable spin state as well as the low temperature lifetime of the metastable state vary strongly from system to system. LIESST and Reverse-LIESST constitute an optical switch, which may eventually lead to practical applications in devices for optical data processing and information storage.

In this review we shall try to introduce the reader into the fascinating field of light-induced spin state conversion in iron(II) complexes leading to long lived metastable states. We shall describe and discuss the most important results which have recently been obtained with various physical techniques. We shall begin, however, with a brief section on the temperature dependent spin transition in iron(II) complexes, since so far LIESST and Reverse-LIESST have only been detected in such complexes.

2. TEMPERATURE DEPENDENT SPIN TRANSITION

2.1 Theoretical Background

Iron(II) is a system with six d-electrons and , according to the simplified Tanabe-Sugano diagram shown in Fig. 1, iron(II) complexes will either have a high spin (HS) $^5T_2$ ground state in a weak ligand field or a low spin (LS) $^1A_1$ ground state in a strong ligand field. If the ligand field strength happens to be in the vicinity of a critical value Δ_{crit}, a thermal spin transition may be observed. In order to understand how this can come about, it is not sufficient to just look at the Tanabe-Sugano diagram. It must be remembered that such a diagram depicts only the electronic energy of the system as a function of the cubic ligand field strength 10Dq, which in turn depends upon the characteristics of the ligand, but, equally important, it is also a strong function of the metal to ligand distance (ref. 11). It is common practice to take 10Dq at the equi-

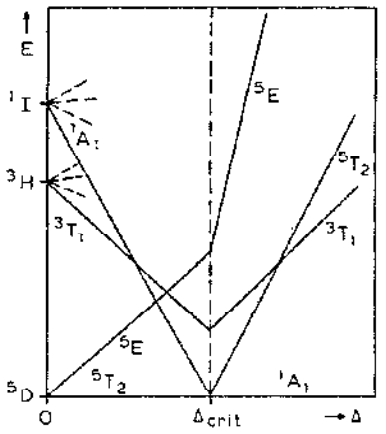

Fig. 1. Simplified Tanabe-Sugano diagram for a d^6-system

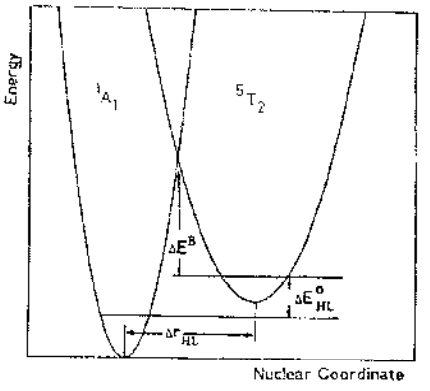

Fig. 2. Relative positions of the HS ($^5T_2$) and LS ($^1A_1$) potential wells in an iron(II) spin crossover compound.

librium nuclear configuration of the ground state as determined from absorption spectra without reference to this fact. But of course we can also determine a 10Dq value appropriate for the equilibrium nuclear configuration of an excited state from emission (ref. 12) or excited state absorption spectra. The crossover point in the Tanabe-Sugano diagram simply means that, for a given ligand, there is a nuclear configuration for which the LS and the HS state are accidentally degenerate. It is clear that this nuclear configuration does not in general correspond to either of the equilibrium configurations, because in iron(II) the LS state with a $(t_2)^6$ configuration generally has shorter metal-ligand bondlengths than the HS state with a $(t_2)^4(e)^2$ configuration by roughly 0.2 Å (ref. 13). Fig. 2 shows the potential wells for the LS and the HS state accordingly. The condition for a thermal spin transition is that ΔE^o_{HL} has to be positive and of the order of k_BT. In this case only the $^1A_1$ state will be populated at low temperatures. At higher temperatures an almost quantitative entropy driven population of the T_2 state will occur, because of the 15-fold electronic degeneracy of the HS state and its higher density of vibrational states.

ΔE^o_{HL} is a complicated function of 10Dq(LS) and 10Dq(HS), which will differ considerably (ref. 9), but also of the force constants in the two potential wells and the difference in metal-ligand bondlength Δr_{HL} between the two states. Any type of argument for the occurrence of spin crossover based only on the static picture of ligand field theory will inevitably lead to misunderstandings.

2.2 Examples and Experimental Techniques

Temperature dependent spin crossover occurs in the crystalline and amorphous solid state as well as in liquid solutions. In the latter case, the molar fraction of complex molecules in the HS state as a function of temperature $\gamma_{HS}(T)$ always follows a simple Boltzmann distribution law for the two states. In the solid state, however, the situation is different. Interactions among the spin state changing metal complexes themselves as well as the complex molecules and the lattice may become very effective, leading to the different shapes for the $\gamma_{HS}(T)$ curves schematically represented in Fig. 3 : gradual (a), abrupt (b), with hysteresis (c), with residual HS fraction at lower temperature and residual LS fraction at higher temperature (d) , with a plateau reflecting a "two-step" transition (e). Many theoretical approaches have been tried by various research groups to describe the different kinds of spin transition behaviour in the solid state (refs. 5,14). Our own contribution to this problem started from the observation that the volume of a complex molecule is considerably larger in the HS state than in the LS state (ref. 13), the difference in the metal- ligand bondlength being ~ 0.2 Å. This causes long-range elastic interactions leading to a cooperative spin transition mechanism (refs. 15,16) . In the following we shall discuss a few solid state spin crossover systems exhibiting various types of spin transition behaviour.

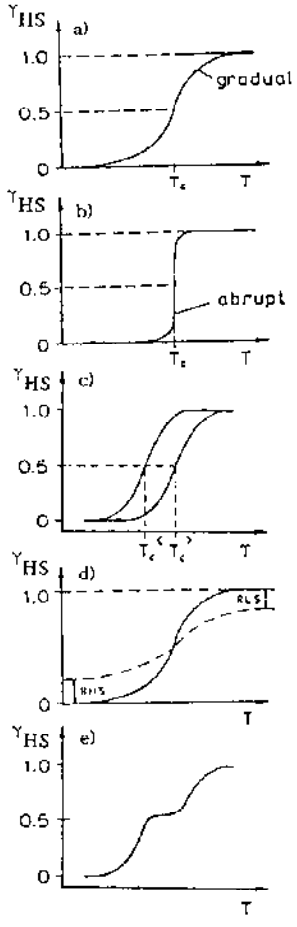

Fig. 3. Various types of spin state transition curves $\gamma_{HS}(T)$ ($\gamma_{HS}(T)$ = molar fraction of HS molecules) occurring in solid state spin crossover systems due to cooperative interactions. a) gradual, b) abrupt, c) with hysteresis, d) with residual HS fraction at lower temperatures and/or residual LS fractions at higher temperatures, e) "two-step" transition.

2.2.1 The $[Fe(2\text{-pic})_3]X_2 \cdot Sol$ System

The spin crossover system we have most extensively studied over a number of years is $[Fe(2\text{-pic})_3]X_2 \cdot Sol$ (2-pic = 2-(aminomethyl)pyridine ; X = Cl, Br; Sol = MeOH, EtOH, H_2O). Early studies using Mössbauer spectroscopy have shown that the HS fraction $\gamma_{HS}(T)$ is a rather steep function of temperature in neat crystals of $[Fe(2\text{-pic})_3]Cl_2 \cdot EtOH$, but becomes increasingly gradual with decreasing iron(II) concentration in the mixed crystal series $[Fe_xM_{1-x}(2\text{-pic})_3]Cl_2 \cdot EtOH$ (refs. 16,17) (see Figs. 4 and 5). This metal dilution effect on the spin transition serves as experimental support for the existence of long-range interactions in the crystals. A quantitative analysis with the "Elastic Interaction and Lattice Expansion Model" (refs. 5,16) can well reproduce the measured $\gamma_{HS}(T)$ curves.

Detailed Mössbauer effect measurements on $[Fe(2\text{-pic})_3]Cl_2 \cdot EtOH$ (ref. 18) revealed that the spin transition, in fact, takes place in two steps, with a plateau at the transition temperature of ~120 K (see Fig. 6). It looks as though the measured $\gamma_{HS}(T)$ curve is the average of two spin transiton curves, $\gamma^{H}_{HS}(T)$ for a predominantly HS lattice with a $T_c(HS)$ = 121 K and $\gamma^{L}_{HS}(T)$ for a predominantly LS lattice with $T_c(LS)$ = 114 K.

The two-step transition in $[Fe(2\text{-pic})_3]Cl_2 \cdot EtOH$ can also be observed by magnetic susceptibility (ref. 18) (Fig. 7) and heat capacity measurements (ref. 19) (Fig. 8). The transition temperatures of all measurements coincide. Sorai et al. obtained a total transition enthalpy of ΔH = 6.14 kJ/mol and a total entropy change of ΔS = 50.6 $J K^{-1}$/mol. These authors suggested that the transition entropy consists of a magnetic contribution, an orientational order-disorder transition of the solvate molecules and the change in the phonon system, primarily due to the change in metal-ligand stretching and deformation vibrations.

Tuchagues et al. (ref. 20) observed a very pronounced plateau in the temperature dependence of $\gamma_{HS}(T)$ of another iron(II) spin crossover system. An even more complicated system with the occurrence of a stepwise spin transition depending upon the temperature cycle was recently described by König et al. (ref. 21).

The spin transition curves and their derivatives as depicted in Fig. 7 for the mixed crystal system $[Fe_xZn_{1-x}(2\text{-pic})_3]Cl_2 \cdot EtOH$ clearly demonstrate that the plateau reduces with decreasing iron concentration and vanishes at $x \approx 0.85$. The appearance of the step seems to be a lattice effect : The step clearly shows up in the temperature dependence of the lattice constants (see Fig. 9) obtained from a variable temperature single crystal X-Ray study. Overall there is a volume change of 61 $Å^3$ per unit cell accompanying the spin transition (ref. 22).

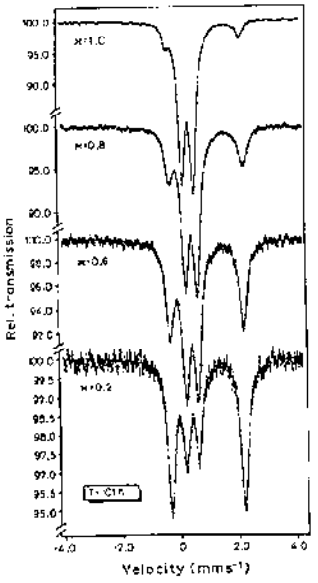

Fig. 4. Concentration dependence of ^{57}Fe Mössbauer spectra at 101 K for mixed crystals $[Fe_xZn_{1-x}(2\text{-pic})_3]Cl_2 \cdot EtOH$ (from ref. 17).

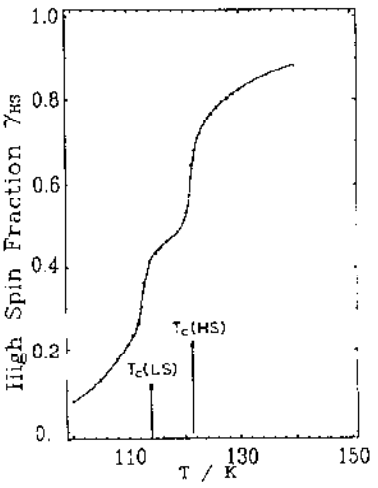

Fig. 6. Temperature dependence of $\gamma_{HS}(T)$ of $[Fe(2\text{-pic})_3]Cl_2 \cdot EtOH$ derived from Mössbauer spectra (integrated area fraction under the resonance lines) (from ref. 18).

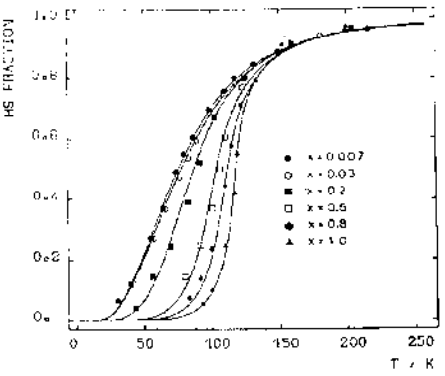

Fig. 5. Temperature dependence of $\gamma_{HS}(T)$ of $[Fe_xZn_{1-x}(2\text{-pic})_3]Cl_2 \cdot EtOH$ with variable iron concentrations. The solid lines were calculated using the "Elastic Interaction and Lattice Expansion" model (from ref. 15).

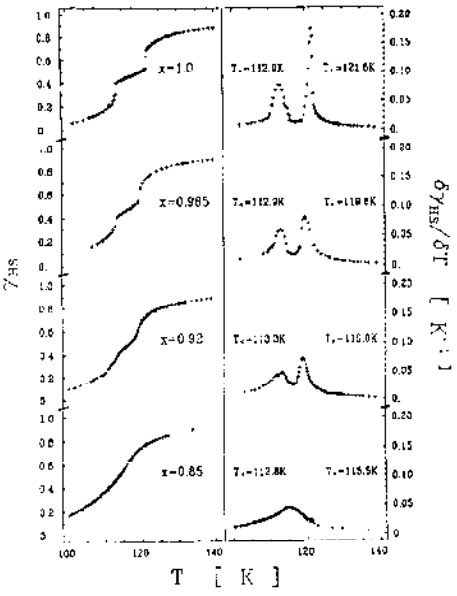

Fig. 7. The effect of metal dilution on the "two-step" spin transition anomaly in $[Fe_xZn_{1-x}(2\text{-pic})_3]Cl_2 \cdot EtOH$ (from ref. 23).

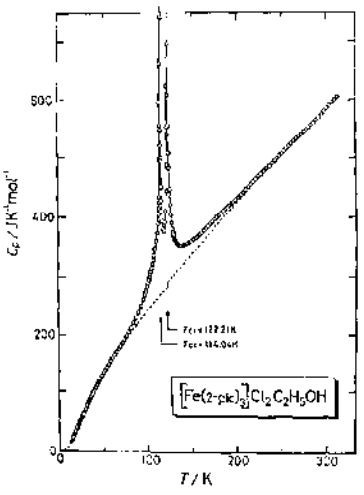

Fig. 8. Molar heat capacity of $[Fe(2\text{-pic})_3]Cl_2 \cdot EtOH$. Broken lines indicate estimated normal heat capacity (from ref. 19).

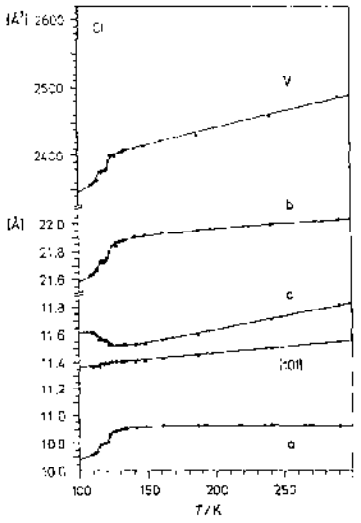

Fig. 9. Temperature dependence of the lattice constants and the unit cell volume of $[Fe(2\text{-pic})_3]Cl_2 \cdot EtOH$. (from ref. 22).

The important role for the spin transition behaviour played by the lattice is also reflected by Fig. 10, where the $\gamma_{HS}(T)$ curves for $[Fe(2\text{-pic})_3]X_2 \cdot EtOH$ for X = Cl and X = Br are compared. The bromide shows a hysteresis in the upper part of $\gamma_{HS}(T)$ and the existence of a plateau is only vaguely perceptible. The effect of anion replacement complements the effect of metal dilution, and again calls for a cooperative spin transition mechanism with long-range elastic interactions. According to the crystal structure (refs. 13,22), the halide anions interconnect the cationic $[Fe(2\text{-pic})_3]^{2+}$ complexes via $-NH_2 \cdots X \cdots H_2N-$ and $-NH_2 \cdots X \cdots HOEt$ hydrogen bonding and thus are actively involved in the interaction pathway from one spin state changing center to another. The phonon system of such an interaction pathway is expected to be altered, whenever the system is modified by any substitution leading to a change in the reduced mass. It is therefore not surprising that the spin transition behaviour changes dramatically if Cl is replaced by Br, even though the crystal structure remains the same.

A drastic change in the spin transition behaviour of $[Fe(2\text{-pic})_3]Cl_2 \cdot Sol$ has also been observed with different crystal solvent molecules, namely EtOH, MeOH, H_2O and 2 H_2O (ref. 24). The solvent molecules are also part of the hydrogen bonding network,

which communicates the information of a spin state change from one metal center to another. The crystal structures of the ethanolate (refs. 25,26), the methanolate and the dihydrate (ref. 27) are different, and one could argue that the difference in the spin transition behaviour comes from this source. However, a careful study of isotopic substitution effects in the $[Fe(2\text{-pic})_3]Cl_2 \cdot EtOH$ system, using Mössbauer spectroscopy, shows that even this subtle modification, which does not change the crystal structure, influences the spin transition strongly (ref. 28). Fig. 11 shows the spin transition curves for $[Fe(2\text{-pic-}ND_2)_3]Cl_2 \cdot C_2H_5OD$ and $[Fe(2\text{-pic-}NH_2)_3]Cl_2 \cdot C_2D_5OH$ together with the undeuterated complex. The effect is only marginal in the case of NH_2/C_2D_5OH deuteration as compared to the undeuterated complex. This is not surprising, since the deuterated positions do not partake in any hydrogen bonding. In case of ND_2/C_2H_5OD deuteration, however, the effect is tremendous : The plateau near T_c has disappeared and the whole $\gamma_{HS}(T)$ curve has moved to higher temperatures with an increase in T_c of ~15 K. In this system the deuterated positions are built into the hydrogen bonds. A similar shift of the $\gamma_{HS}(T)$ curve has been observed in the deuterated methanolate $[Fe(\text{-}2\text{-pic-}ND_2)_3]Cl_2 \cdot CH_3OD$ as compared to the protonated system (ref. 29).

The effect of isotopic substitution $^{14}N/^{15}N$ at the amino group is clearly seen in Fig. 12. Although the nitrogen atom of the amino group is an active member of the hydrogen bonding pathway the effect is relatively small because of the small difference in mass.

The effects of metal dilution, anion replacement, different crystal solvent molecules, isotopic exchange, and their specific influence on the spin transition characteristics arise from lattice interactions in one way or another. From the fact that the volume of the individual complex molecule (refs. 13,22) and thus the unit cell volume decreases sharply on going from the HS to the LS phase, we expect that application of pressure should favour the stabilization of the LS phase. This has indeed been observed by a number of research groups for various iron(II) spin crossover systems (refs. 30-33). Applying pressure to polycrystalline material of $[Fe(2\text{-pic})_3]Cl_2 \cdot EtOH$ removes the plateau in $\gamma_{HS}(T)$ and shifts the whole curve to higher temperatures (refs. 33,34) (see Fig. 13) by approximately 15 K.

McCusker et al. (ref. 32) have recently performed pressure studies on $[Fe(dppen)_2X_2]$ (dppen = cis-1,2-bis(diphenylphosphino)ethylene; X = Cl, Br) and concluded that lattice cooperativity in addition to ligand field and polarizability effects are responsible for the observed differences in transition pressures between the dichloro and the dibromo complexes.

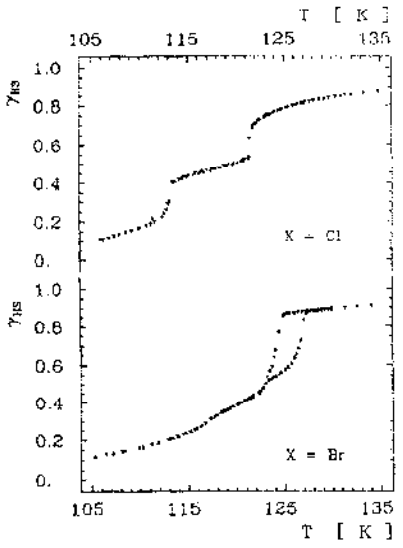

Fig. 10. Temperature dependence of $\gamma_{HS}(T)$ derived from magnetic susceptibility measurements for $[Fe(2\text{-pic})_3]X_2 \cdot EtOH$ (X = Cl, Br) (from ref. 23).

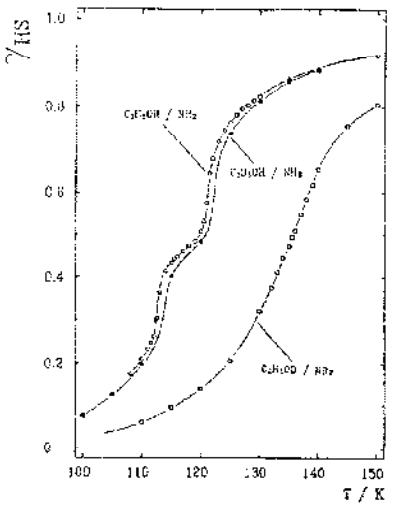

Fig. 11. Effect of H/D exchange on the temperature dependence of $\gamma_{HS}(T)$ of $[Fe(2\text{-pic})_3]Cl_2 \cdot EtOH$ from Mössbauer measurements (from ref. 26).

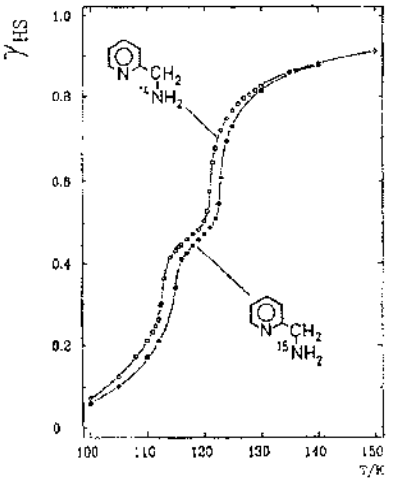

Fig. 12. Effect of $^{14}N/^{15}N$ exchange in the amino group of the ligand on $\gamma_{HS}(T)$ of $[Fe(2\text{-pic})_3]Cl_2 \cdot EtOH$ from Mössbauer measurements (from ref. 28).

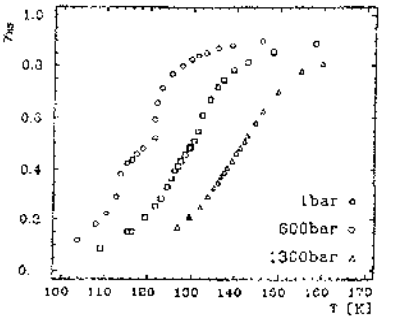

Fig. 13. Temperature dependence of $\gamma_{HS}(T)$ of $[Fe(2\text{-pic})_3]Cl_2 \cdot EtOH$ as a function of applied pressure (from ref. 34).

2.2.2 The $[Fe(Rtz)_6](BF_4)_2$ System

Iron(II) complexes of the type $[Fe(Rtz)_6](BF_4)_2$ (Rtz = 1-alkyltetrazole) have been found to exhibit a temperature dependent spin transition (refs. 35,36). Fig. 14 shows three representative Mössbauer spectra of $[Fe(ptz)_6](BF_4)_2$ (ptz = 1-propyltertrazole) which were recorded in our laboratory : The spectrum at 160 K is characteristic for the HS phase (the pronounced difference in the line intensities of the HS quadrupole doublet is due to texture), the one at 80 K for the LS phase and the one in between for a mixture of both near the transition temperature of $T_c \approx 133$ K. The spin transition is accompanied by a first order phase transition as can be seen from Fig. 15: The effective magnetic moment as a function of temperature shows a hysteresis of ~7 K (ref. 9). At room temperature this compound is colourless, and the optical spectrum shows just a weak $^5T_2 \rightarrow {}^5E$ absorption band in the near infrared (see Fig. 16a) . Below the transition temperature the crystals become deeply purple , the weak quintet-quintet band disappears and instead two new bands in the visible appear , corresponding to the spin-allowed d-d transitions $^1A_1 \rightarrow {}^1T_1$ and $^1A_1 \rightarrow {}^1T_2$. In the dilute material $[Fe_xZn_{1-x}(ptz)_6](BF_4)_2$ ($x \approx 0.1$) the spin transition is gradual and a value for ΔE^o_{HL} of ~ 500 cm^{-1} can be estimated from the temperature dependence of the $^1A_1 \rightarrow {}^1T_1$ absorption band (ref. 37).

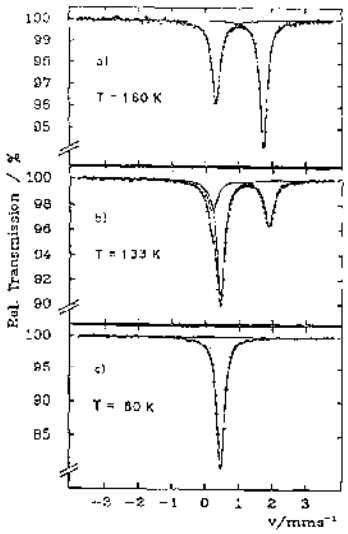

Fig. 14. ^{57}Fe Mössbauer spectra of $[Fe(ptz)_6](BF_4)_2$ a) above T_c, b) near T_c) and c) below T_c

In the analogous complex compound $[Fe(mtz)_6]X_2$ (mtz = 1-methyltetrazole, X = ClO_4 , BF_4) the iron(II) complexes occupy two slightly different lattice sites (ref. 38) The Mössbauer spectra arising from the two sites are identical at room temperature with typical parameters for iron(II) in the HS state (see Fig. 17). Only below ~160 K the two sites become distingulsbable. We shall denote the site with the smaller

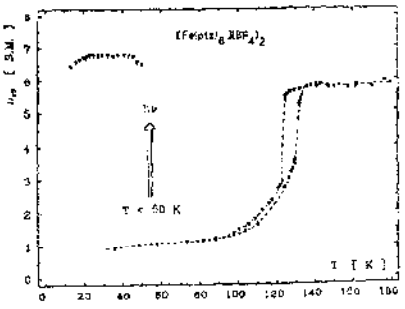

Fig. 15. Effective magnetic moment μ_{eff} of $(Fe(ptz)_6](BF_4)_2$ as a function of temperature. The hysteresis of ~7 K is typical for a first order phase transition accompanying the spin transition. After the irradiation with green light below ~50 K a value of 6.5 μ_B for μ_{eff} was obtained, indicating that LS→ HS conversion has taken place. (from ref. 9).

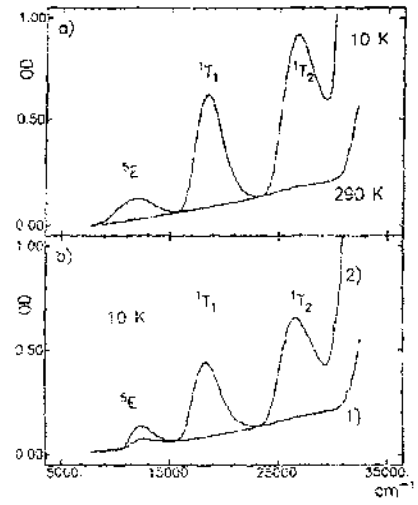

Fig 16. Single-crystal absorption spectra in the region of d-d transitions of $(Fe(ptz)_6](BF_4)_2$ (π-polarisation). a) Temperature dependence, b) after irradiation at 514.5 nm at 10 K (1) and subsequent irradiation at 752.5 nm (2) (adapted from refs. 9,10).

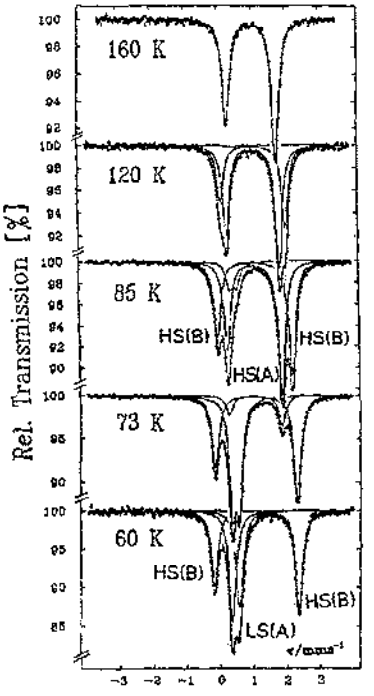

Fig. 17 ^{57}Fe Mössbauer spectra of $(Fe(mtz)_6](BF_4)_2$ at selected temperatures (from ref. 39).

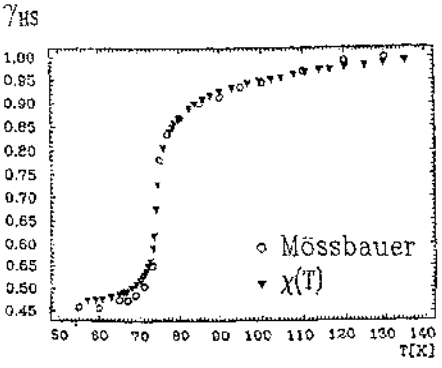

Fig. 18. HS fraction $\gamma_{HS}(T)$ as a function of temperature for $(Fe(mtz)_6](BF_4)_2$ derived from Mössbauer spectra and magnetic susceptibility measurements (from ref. 39).

quadrupole doublet (inner two lines) as site A; correspondingly we shall refer to the outer lines as to the quadrupole doublet arising from site B. Only iron(II) complexes on site A undergo a thermal spin transition with a transition temperature $T_c \approx 75$ K. Below T_c the Mössbauer spectra consist of the LS(A) quadrupole doublet from site A with only a small splitting and the HS(B) quadrupole doublet of site B. The HS fraction $\gamma_{HS}(T)$ as a function of temperature derived from the Mössbauer spectra (normalized integrated area of the resonance lines) coincides with the one obtained from magnetic susceptibility measurements (ref. 39) (see Fig. 16). Note that at low temperatures $\gamma_{HS}(T)$ tends towards a value of 0.5 due to the fact that B- site iron(II) complexes remain in the HS state. The rather low transition temperature $T_c \approx 75$ K for site A complexes indicates that $\Delta E^o_{HL}(A)$ is small and positive. The fact that the B-site complexes remain in the HS state means that $\Delta E^o_{HL}(B)$ is close to zero and could even be negative.

3. LIGHT-INDUCED EXCITED SPIN STATE TRAPPING (LIESST)

In the course of our investigations of thermally driven spin transitions in iron(II) complex compounds we observed a fascinating photophysical effect : at low temperatures the thermodynamically stable LS state can be converted quantitatively to a metastable HS state by irradiating into the $^1A_1 \rightarrow {}^1T_1$ absorption band. At low temperatures the system remains trapped in this HS state with a practically infinite lifetime. We have called this phenomenon "Light-Induced Excited Spin State Trapping (LIESST)" (refs. 8, 9).

3.1 First Observations of LIESST

We first observed LIESST in $[Fe(ptz)_6](BF_4)_2$, the thermal spin crossover behaviour and the absorption spectra of which were discussed in 2.2.2. Irradiating a single crystal at 10 K, where it is in the purple LS state, with the 514.5 nm line of an Ar^+laser completely bleached it within a few tens of seconds. The absorption spectrum at 10 K after the irradiation is identical to the typical HS spectrum recorded at 290 K (see Fig. 16b). That at 10 K this metastable state is indeed a HS state can be confirmed by magnetic susceptibility measurements (see Fig. 15) as well as Mössbauer spectroscopy (ref. 8). LIESST has also been observed in the dilute material $[Fe_xZn_{1-x}(ptz)_6](BF_4)_2$ ($x \sim 0.1$), indicating that it is basically a single ion process (ref. 10, 37).

3.2 Mechanism for LIESST

The mechanism for LIESST can be explained on the basis of Fig. 19 : Irradiating the cold sample with the 514.5 nm line of an Ar^+ laser induces spin-allowed $^1A_1 \rightarrow {}^1T_1$ transitions. The excited singlet state is short-lived and can quickly decay back to the ground state. There is, however, an alternative decay path, made possible by spin-orbit coupling, which enables an intersystem crossing step with $\Delta S = 1$ to the triplet states $^3T_1$ and $^3T_2$. These in turn decay via a second intersystem crossing step either to the $^1A_1$ ground state or to the metastable $^5T_2$ state. The system remains trapped in the HS state with a very long lifetime as long as the temperature is low enough, so that the energy barrier between the HS and LS potential surfaces, which are well separated by the large difference in metal-ligand bondlength, cannot be overcome thermally. The radiationless intersystem crossing steps, except for the $HS(^5T_2) \rightarrow LS(^1A_1)$ relaxation, are fast (on the nanosecond timescale), so if we keep on irradiating into the $^1A_1 \rightarrow {}^1T_1$ absorption band eventually all complexes will end up in the long-lived HS state.

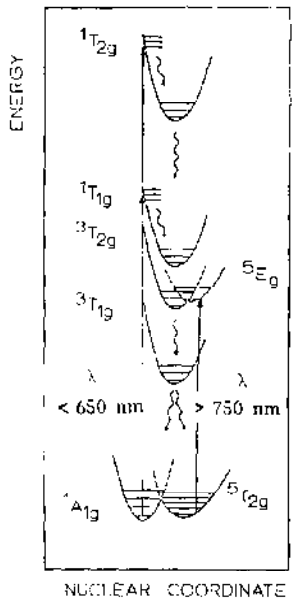

Fig. 19. Schematic representation of the potential wells of the excited ligand field states in a d^6 spin crossover system. Arrows indicate the mechanism for LIESST and reverse-LIESST (from ref. 9)

3.3 Reversibility of LIESST

Crucial for the mechanism of LIESST is the low lying $^3T_1$ state which acts as an intermediate in the two step intersystem crossing. Unfortunately it is rather elusive spectroscopically, but ligand field calculations (ref. 9) put it to well below the $^1T_1$ state and even to below the ^5E state, as indicated in Fig. 19. In this case it should be possible to pump the trapped HS state back to the LS state by irradiating into the $^5T_2 \rightarrow {}^5E$ absorption band in the near infrared. That this is indeed the case is borne out

by Fig. 16b, where the absorption spectra of $[Fe(ptz)_6](BF_4)_2$ after a first irradiation at 514.5 nm leading to the metastable HS state and subsequent irradiation at 752.5 nm (Kr^+laser) at 10 K are shown. The system can in fact be cycled back and forth any number of times, using light of the appropriate wavelength. In the neat compound the light-induced HS-LS conversion is not quite quantitative, in the dilute material $[Fe_xZn_{1-x}(ptz)_6](BF_4)_2$ (x ~ 0.1) it is complete (ref. 10).

3.4 LIESST in the $[Fe(mtz)_6](BF_4)_2$ System

Site A in $[Fe(mtz)_6](BF_4)_2$ behaves very much like the ptz system : Irradiation at ~20 K with $\lambda < 650$ nm converts the LS(A) state quantitatively to the metastable HS(A) state. In the Mössbauer spectrum the LS(A) doublet disappears completely in favour of the HS(A) doublet. The HS(B) doublet is not affected (see Fig. 20) (ref. 40). The metastable HS(A) state has a practically infinite lifetime at ~20 K. Only above ~45 K does thermal relaxation set in. Irradiation with $\lambda > 750$ nm reconverts the HS(A) state back to the LS(A) state, with just a small fraction of site A molecules remaining in the HS state. In addition, however, the site B complexes get converted from the thermodynamically stable HS(B) state to a now metastable LS(B) state (metastable because $\Delta E^{o}_{HL}(B) \leq 0$) , again with a small fraction of site B ions remaining in the HS state (see Fig. 21) . The metastable LS(B) state too has a very long lifetime at ~20 K . Thermal relaxation to the HS(B) state is observed above ~ 55 K. This is the first example of an iron(II) complex, where the thermodynamically stable HS state could be converted into a metastable LS state with light. The observation that the HS(B) → LS(B) conversion is not quite quantitative and that simultaneously a fraction of A-site

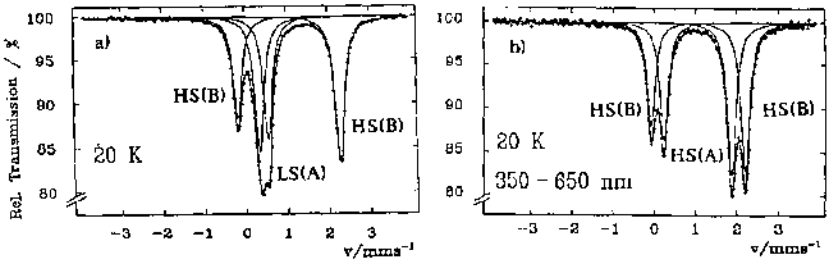

Fig. 20. ^{57}Fe Mössbauer spectra of $[Fe(mtz)_6](BF_4)_2$ at 20 K before (a) and after (b) irradiation with green light ($\lambda < 650$ nm). The LS(A) state is quantitatively converted to the HS(A) state (from ref. 40).

complexes undergo a LS(A) → HS(A) conversion under irradiation in the near infrared (λ > 750 nm) is a consequence of the broad-band irradiation (Xe lamp and filters) and an overlap of the $^1A_1 \rightarrow {}^1T_1$ and the $^5T_2 \rightarrow {}^5E$ absorption bands.

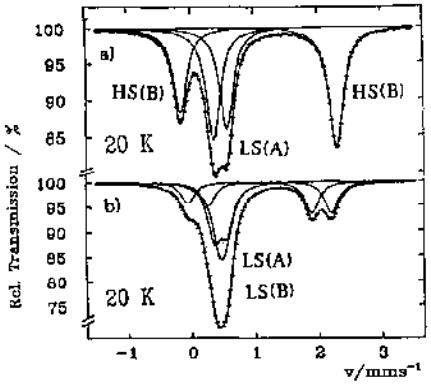

Fig. 21. ^{57}Fe Mössbauer spectra of $[Fe(mtz)_6](BF_4)_2$ at 20 K before (a) and after (b) irradiation with near infrared light (λ > 750 nm). ~75% of B-site complexes are converted from the HS(B) to the LS(B) state. A small fraction of A-site complexes is simultaneously converted from the LS(A) to the HS(A) state (from ref. 39).

3.5 LIESST in other Iron(II) Spin Crossover Systems

LIESST is not unique to $[Fe(ptz)_6](BF_4)_2$ and related systems , nor is it restricted to crystalline materials. Since the discovery of LIESST in 1984, long-lived metastable HS states have been found in a number of iron(II) spin crossover compounds : $[Fe(2\text{-pic})_3]X_2 \cdot EtOH$ (X = Cl, Br) (ref. 9) and $[Fe_xZn_{1-x}(2\text{-pic})_3]Cl_2 \cdot EtOH$ (x ≈ 0.0003) (ref. 41), $[Fe(bipy)_2](NCS)_2]$ (ref. 42), $[Fe(phen)_2](NCS)_2]$ (ref. 43), $[Fe(2\text{-mephen})_3](ClO_4)_2$ (ref. 44) , all in the solid state, and $[Fe(2\text{-mephen})_3](ClO_4)_2$ embedded in poly-vinyl acetate (PVAc) and Nafion ion exchange foils (ref. 45), to name but a few. In all of the above compounds the HS LS relaxation rate at ~10 K is less than 10^{-4} s^{-1}. There is, however, a difference between these and the Rtz systems : In these compounds the LS d-d absorption bands are obscured by low-lying MLCT bands. Fig. 22a shows the temperature dependence of this MLCT band of $[Fe(2\text{-mephen})_3](ClO_4)_2$ embedded in PVAc. Because of the shorter M-L bondlength in the LS state the overlap between metal and ligand centered orbitals is much larger than in the HS state, resulting in a higher intensity of the MLCT band in the LS state. Irradiation at 514.5 nm , i.e. into the MLCT band , at ~ 10 K produces a long-lived HS state : After the irradiation the absorption spectrum is identical to the high temperature spectrum, typical for the HS state (see Fig. 22b). In this case thermal HS → LS relaxation becomes noticeable at

temperatures above ~50 K, however, with a strong deviation from first order kinetics, probably due to local inhomogeneities in the polymer films.

From the fact that LIESST is observed in crystalline materials (both neat and dilute) as well as in iron(II) complexes dispersed in amorphous matrices, we conclude that it is quite a common phenomenon in spin crossover compounds and, more importantly, that it is basically a property of a single complex.

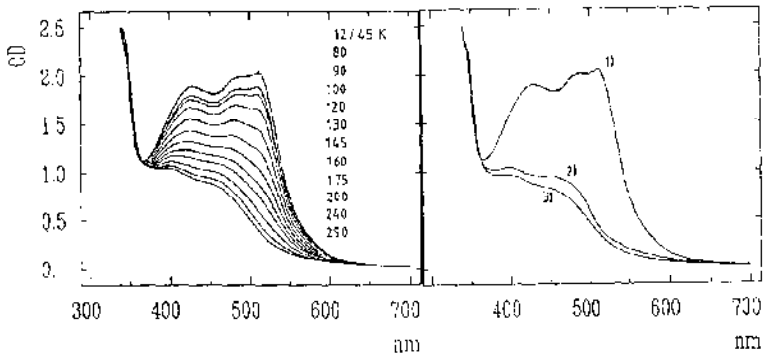

Fig. 22. (a) Variable temperature absorption spectra of $[Fe(2\text{-mephen})_3](ClO_4)_2$ embedded in poly-vinylacetate (PVAc), showing the increase in intensity of the MLCT band at low temperatures, where the complex is in the LS state. (b) Absorption spectra of $[Fe(2\text{-mephen})_3](ClO_4)_2$ embedded in PVAc at 12 K before irradiation (1) and after irradiation (2) at 514.5 nm. For comparison the 290 K spectrum is included (from ref. 45).

4. DYNAMICS OF SPIN STATE CONVERSION

The dynamics of spin state conversion in solution at ambient temperatures has been the subject of a number of papers over the last two decades (refs. 46-50). Techniques used were photoperturbation and transient absorption , Raman-laser temperature jump and ultrasonic relaxation. It was in fact McGarvey and Lawthers (ref. 49) who were the first to notice a rapid depopulation of the LS state upon pulsed laser irradiation in an iron(II) spin crossover complex in solution. The measured HS → LS relaxation rates k_{HL} were of the order of 10^7 s^{-1} and the results were explained in terms of conventional transition state theory. A full account may be found in a recent review by Beattie (ref. 7).

A lot less is known about LS ⇄ HS relaxation in the solid state and at low temperatures , particularly in the case of iron(II) spin crossover complexes. Mössbauer lineshape analysis can be used to determine rate constants in the range of 10^6 - 10^8 s^{-1}, provided both spin states are present in appreciable amounts. High temperature rates

of the same order of magnitude as in solution were found in a number of suitable compounds (refs. 51,52).

From photoperturbation (i.e. LIESST) and temperature quenching experiments (refs. 21,53,54) we know that for iron(II) spin crossover complexes HS → LS relaxation rates at low temperatures can become very much smaller both in crystalline material as well as embedded in amorphous matrices.

4.1 Thermal HS → LS Relaxation in $[Fe_xZn_{1-x}(ptz)_6](BF_4)_2$

At 10 K the HS → LS relaxation rate k_{HL} in $[Fe_xZn_{1-x}(ptz)_6](BF_4)_2$ is less than 10^{-6} s^{-1}. Only above ~ 60 K does the trapped HS state begin to decay. Due to cooperative effects (long-range elastic forces) in the neat material the decay is highly non-exponential, but in the dilute material with $x \approx 0.1$ the decay is exponential and from an $\ln(k_{HL})$ vs. 1/T plot an activation energy ΔE^a of ~ 800 cm^{-1} and a frequency factor A of ~ 10^5 s^{-1} can be obtained (ref. 37). As Beattie (ref. 7) pointed out, one should be careful in making direct comparisons with room temperature data. However, we can try and estimate the classical energy barrier ΔE^B between the LS and the HS potential wells. We know ΔE^o_{HL} and Δr_{HL} to be ~ 500 cm^{-1} and 0.2 Å respectively. If we assume a metal-ligand force constant f ~ 1.7×10^5 dyn/cm – this is slightly larger than in the high-spin iron(II) hexaaquo complex (ref. 55) – we get ΔE^B ~ 2000 cm^{-1}. This is quite considerably larger than the experimental activation energy ΔE^a, a first indication that classical concepts are not adequate in discribing the dynamics of spin state conversion.

4.2 HS → LS Relaxation in $[Fe_xZn_{1-x}(2\text{-pic})_3]Cl_2$ Sol , $[Fe(mepy)_2(py)(tren)](PF_6)_2$ in PSS , $[Fe(phen)_3](CLO_4)_2$ in Nafion and $[Fe_xZn_{1-x}(bipy)_3](PF_6)_2$

Xie and Hendrickson (ref. 56) have measured the excited state lifetime as a function of temperature in the spin crossover compound $[Fe(mepy)_2(py)(tren)](PF_6)_2$ embedded in poly-styrene sulfonate (see Fig. 23) using the photoperturbation technique. Below ~ 80 K they found an only weakly temperature dependent relaxation rate of ~ 10^4 s^{-1}, evidence for nuclear tunnelling. Above ~ 100 K a thermally activated process becomes dominant with an experimental activation energy ΔE ~ 800 cm^{-1}. The question now is ,what are the parameters which govern the excited state lifetime, leading to a low temperature tunnelling rate of less than 10^{-6} s^{-1} in one case and 10^4 s^{-1} in another ? Is there a smooth transition from the one case to the other, or do the compounds fall

into classes ? Well, in a number of spin crossover compounds we investigated a light-induced population of metastable HS states was possible, but with 10^{-1} to 10^{-3} s^{-1} even below 10 K the low temperature relaxation rates were considerably larger than the $< 10^{-6}$ s^{-1} in the classic LIESST compound $[Fe(ptz)_6](BF_4)_2$. Among the systems studied were $[Fe(mepy)_3(tren)](PF_6)_2$ dispersed in KBr, Nafion and PMMA (ref. 57) and $[Fe_xZn_{1-x}(2\text{-pic})_3]\,Cl_2 \cdot MeOH$. In Fig. 23 the relaxation rate k_{HL} as a function of temperature for the latter system is shown (refs. 41, 52). In the low temperature region the photoperturbation technique was used for samples with x = 0.0003 , in the high temperature region the rates were determined from linshape analysis of Mössbauer spectra for samples with x = 1. Qualitatively the result is similar to the one obtained by Xie and Hendrickson for their system : Arrhenius type behaviour at high temperatures with $\Delta E^a \approx 1000$ cm^{-1} but a somewhat smaller tunnelling rate of 10^{-2} s^{-1} at low temperatures.

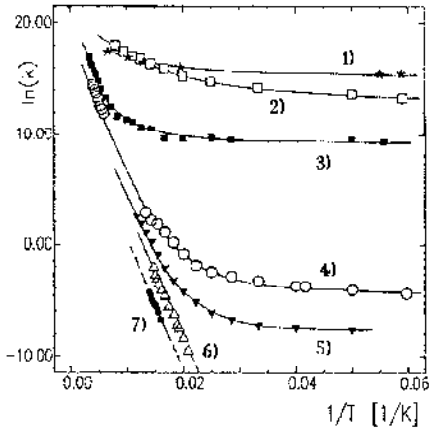

Fig. 23. HS → LS relaxation rates as function of temperature for a number of iron(II) complexes:
1) $[Fe(phen)_3](ClO_4)_2$ in Nafion (ref. 57) low-spin
2) $[Fe_xZn_{1-x}(bipy)_3](PF_6)_2$ $x \approx 0.0005$ (ref. 57) low-spin
3) $[Fe(mepy)_2(py)(tren)](PF_6)_2$ in PSS (ref. 56) $T_c > 300$ K
4) $[Fe_xZn_{1-x}(2\text{-pic})_3]Cl_2 \cdot MeOH$ $x \approx 0.0003$ (refs. 41, 52) $T_c = 180$ K
5) $[Fe_xZn_{1-x}(2\text{-pic})_3]Cl_2 \cdot EtOH$ $x \approx 0.0003$ (ref. 41) $T_c = 80$ K
6) $[Fe(2\text{-mephen})_3](ClO_4)_2$ in Nafion (ref. 45) $T_c = 120$ K
7) $[Fe_xZn_{1-x}(ptz)_6](BF_4)_2$ $x \approx 0.1$ (ref. 37) $T_c = 100$ K

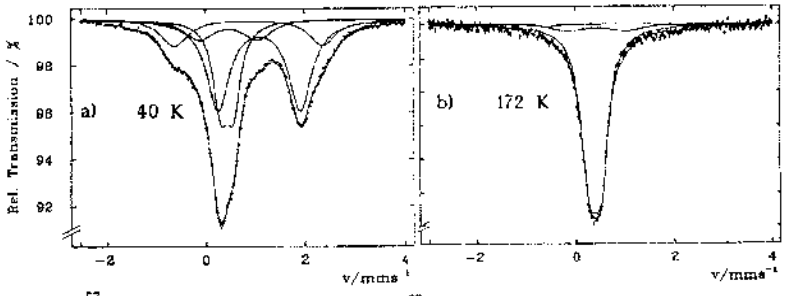

Fig. 24. ^{57}Co Mössbauer emission spectra of $[^{57}Co/Co(phen)_3](ClO_4)_2$ a) at 40 K, b) at 172 K (from ref. 58).

Included in Fig. 23 are the HS→LS relaxation rates for two typical low-spin compounds, namely $[Fe(phen)_3](ClO_4)_2$ embedded in Nafion and $[Fe_xZn_{1-x}(bipy)_3](PF_6)_2$ (x = 0.0005) (ref. 57). In both compounds a transient population of the HS state can be achieved. The relaxation rates shown in Fig. 23 were obtained with the photoperturbation and transient absorption technique. That we are indeed looking at HS states is borne out by Fig. 24 which shows the ^{57}Co Mössbauer emission spectrum of $[^{57}Co/Co(phen)_3](ClO_4)_2$. At 40 K the spectrum consists of both LS and HS doublets, indicating that after the ^{57}Co (EC) ^{57}Fe process at least some of the iron(II) complexes end up in the HS state with a lifetime of the order of the characteristic Mössbauer time of 10^{-7} s or larger . At 172 K only the LS doublet remains, as is to be expected since the HS → LS relaxation rate at that temperature is larger than 10^8 s^{-1} (ref. 58).

4.3 Nonadiabatic Multiphonon Relaxation

From the examples in 4.2. we conclude that the low temperature tunnelling rate from the excited HS state to the LS ground state can vary smoothly between 10^{-6} s^{-1} in $[Fe(ptz)_6](BF_4)_2$ and 10^7 s^{-1} for $[Fe(phen)_3](ClO_4)_2$. The fact that tunnelling is observed at low temperatures and that the apparent activation energies at higher temperatures are much lower than expected from a classical picture indicates that the HS → LS relaxation is highly nonadiabatic.

Buhks et al. (ref. 59) described "HS → LS relaxation in transition metal complexes in terms of a radiationless nonadiabatic multiphonon process occurring between two distinct zero-order spin states characterized by different nuclear configurations". For iron(II) with ΔS = 2 only higher order spin-orbit coupling can mix the two states. Starting from Fermi's Golden Rule and using the Born-Oppenheimer approximation the intersystem crossing rate can be expressed as:

$$k_{H\rightarrow L}(T) = \frac{2\pi}{\hbar} g_f \beta_{HL}^2 G(T) \quad ,$$

where g_f = 1 is the electronic degeneracy of the final state , $\beta_{HL} \approx 150$ cm^{-1} is the electronic matrix element and G(T) is a thermally averaged nuclear Frank-Condon vibrational overlap factor. Buhks et al. (ref. 59) derived an analytical expression for G(T), making the following assumptions : a) only one internal vibrational mode, namely the totally symmetric vibration, with frequency ω_k and displacement δQ_k contributes to G(T), b) frequency changes between the HS and the LS are neglected and c) medium modes just provide the continuous phonon spectrum required to ensure energy conser-

vation, but are otherwise ignored. G(T) is a strong function of the reduced energy gap $\Delta E^{o}_{HL}/\hbar\omega_k$ and the Huang-Rhys parameter $S = \frac{1}{2} f_k (\Delta Q_k)^2 / \hbar\omega_k = \frac{1}{2} \mu_k (\Delta Q_k)^2 / \hbar$, that is the vertical and horizontal displacements of the two potential wells relative to each other. The general features of $k_{H\rightarrow L}(T)$ according to Buhks et al. (ref. 59) are a temperature independent tunnelling rate at low temperatures and an activated relaxation process at higher temperatures, with an apparent activation energy which is much lower than the classical energy barrier, i. e. at elevated temperatures the relaxation is still nonadiabatic, tunnelling occurs from an excited vibrational state.

For $[Fe(ptz)_6](BF_4)_2$ we know $\Delta Q_k = \sqrt{6}\,\Delta r_{HL} \approx 0.5$ Å and $\omega_k \approx 250$ cm^{-1} from X-ray crystallography and vibrational spectroscopy respectively, and $\Delta E^{o}_{HL} \approx 500$ cm^{-1} from the thermal spin transition. The main difficulty in estimating S lies in the force constant f_k and the reduced mass μ_k. Taking just the mass of the coordinating atom clearly underestimates μ_k and results in an unrealistically small force constant f_k. We have therefore chosen $f_k \sim 1.7 \times 10^5$ dyn/cm as a realistic value for f_k. This is slightly larger than the force constant for the totally symmetric vibration in the high-spin iron(II) hexaaquo complex (ref. 55). With these values we estimate $S \sim 50$ and the resulting low temperature tunnelling rate is $\sim 10^{-4}$ s^{-1}. This is in the range needed to explain our extremely long-lived excited states at least semi-quantitatively.

In all the iron(II) complexes we have considered so far the central atom is surrounded by six nitrogen atoms belonging to mainly aromatic ligands. It is a fair assumption that Δr_{HL} and f_k and therefore S will not vary to any great extent within this class of compounds. What will vary is the energy gap and the frequency of the accepting mode. An increase in ΔE^{o}_{HL} immediatly results in a much faster low temperature tunnelling rate in accordance with experiment. In Fig. 23 T_c, which is a crude measure for the energy gap, is given for the various compounds. With an energy gap $\Delta E^{o}_{HL} > 2500$ cm^{-1} in the case of low-spin compounds, such as the $[Fe(phen)_3](ClO_4)_2$ and $[Fe(bipy)_3](PF_6)_2$ systems the estimated low temperature tunnelling rate is of the order of 10^7 s^{-1}.

The nonadiabatic multiphonon relaxation, a fully quantum mechanical approach, is able to explain the general features of HS → LS relaxation in iron(II) compounds, and order of magnitude estimates of the low temperature tunnelling rate are in fair agreement with observation. It would, however, be presumptuous to expect a more quantitative interpretation from the single mode calculation. At low temperatures neglecting the low energy phonon dispersion is critical, at elevated temperatures it is the assumption that there is no frequency change in the active vibration on going from HS to LS which is not really valid.

Acknowlegement

We wish to thank our collaborators and students who have contributed to our spin crossover and LIESST research. P. Poganiuch, A. Vef and C. Hennen have made available results prior to publication. Particular thanks are extended to the Bundesministerium für Forschung und Technologie, the Deutsche Forschungsgemeinschaft, the Fonds der Chemischen Industrie, and the University of Mainz for financial support.

References

1 L. Cambi, L. Szegö, A. Cassano, Acad. Naz. Lincei 15 (1932b) 329.
2 W. A. Baker, H. M. Bobonich, Inorg. Chem 20 (1965) 1184
3 R. L. Martin, A. H. White, in Transition Metal Chemistry, Vol. **4**, (R. L. Carlin, ed.) Marcel Dekker Inc. ,New York 1968, p. 113.
4 H. A. Goodwin, Coord. Chem. Rev. **18**, 293 (1976).
5 P. Gütlich, Structure and Bonding **44**, 83 (1981).
6 E. König, G. Ritter, S. K. Kulshreshtha, Chem. Rev. 85, 219 (85).
7 J. K. Beatty, Adv. Inorg. Chem. **32**, 1 (1988).
8 S. Decurtins , P. Gütlich, C. P. Köhler, H. Spiering, A. Hauser, Chem. Phys. Lett. **105** (1984) 1.
9 S. Decurtins, P. Gütlich, K. M. Hasselbach, A. Hauser, H. Spiering, Inorg. Chem. **24** (1985) 2174.
10 A. Hauser, Chem. Phys. Lett. **124** (1986) 543.
11 H. L. Schläfer, G. Glieman , Einführung in die Ligandenfeldtheorie, Akad. Verlagsgesellschaft, 1980.
12 R. B. Wilson, E. I. Solomon, Inorg. Chem 17 (1978) 1729.
13 M. Mikami, M. Konno, Y. Saito, Acta Cryst. **B36** (1980) 275.
14 C. N. Rao, Int. Rev. Phys. Chem. **4** (1985) 19.
15 H. Spiering, E. Meissner, H. Köppen, E. W. Müller, P. Gütlich, Chem. Phys. **68** (1982) 65.
16 P. Adler, L. Wiehl, E. Meissner, C. P. Köhler, H. Spiering, P. Gütlich, J. Phys. Chem. Solids **48** (1987) 517.
17 M. Sorai, J. Ensling, P. Gütlich, Chem. Phys. Lett. **18** (1976) 199.
18 H. Köppen, E. W. Müller, C. P. Köhler, H. Spiering, E. Meissner, P. Gütlich, Chem. Phys. Lett. **91** (1982) 348.
19 K. Kaji, M. Sorai, Thermochim. Acta **88** (1985) 185.
20 V. Petrouleas, J.-P. Tuchagues, Chem. Phys. Lett. **137** (1987) 21.
21 E. König, G. Ritter, J. Dengler, S. M Nelson, Inorg. Chem. 26 (1987) 3582.
22 L. Wiehl, G. Kiel, C. P. Köhler, H. Spiering, P. Gütlich, Inorg. Chem. **25** (1986) 1565.
23 C.P. Köhler, P. Gütlich, unpublished results.
24 M. Sorai, J. Ensling, K. M. Hasselbach, P. Gütlich, Chem. Phys. 20 (1977) 197.

25 M. Mikami, M. Konno, Y. Saito, Chem. Phys. Lett. **63** (1979) 566.

26 B. A. Katz, C. E. Strouse, J. Am. Chem. Soc. **101** (1979) 6214.

27 A. M. Greenaway, E. Sinn, J. Am. Chem. Soc. **100** (1978) 8080.

28 H. Köppen, Ph. D. Thesis, Fachbereich Chemie und Pharmazie, Universität Mainz, 1985.

29 P. Gütlich, H. Köppen, H. G. Steinhäuser, Chem. Phys. Lett. **74** (1980) 475.

30 H. G. Drickamer, C. W. Frank, Electronic Transitions and the High Pressure Chemistry and Physics of Solids, Chapman and Hall, London 1973.

31 G. J. Long, B. B. Hutchinson, Inorg. Chem. **26** (1987) 608.

32 J. K. McCusker, M. Zvagulis, H. G. Drickamer, D. N. Hendrickson, Inorg. Chem. **28** (1989) 1380.

33 E. Meissner, H. Köppen, H. Spiering, P. Gütlich, Chem. Phys Lett. **95** (1983) 163.

34 E. Meissner, Ph.D. Thesis, Fachbereich Physik, Universität Mainz, 1984.

35 P. L. Franke, W. L. Groeneveld, Transition Met. Chem. **6** (1981) 6.

36 P. L. Franke, J. G. Haasnoot, A. P. Zuur, Inorg. Chim. Acta **59** (1982) 5.

37 A. Hauser, P. Gütlich, H. Spiering, Inorg. Chem **25** (1986) 4245.

38 L. Wiehl, to be published.

39 P. Poganiuch, P. Gütlich, submitted to J. Amer. Chem. Soc.

40 P. Poganiuch, P. Gütlich, Hyperfine Inter. **40** (1988) 331.

41 A. Vef. , Diplomarbeit , Universität Mainz , 1988.

42 S. Decurtins, P. Gütlich, C. P. Köhler, H. Spiering, J. Chem. Soc. Chem. Commun. 1985, 430.

43 R. Herber, Inorg. Chem. **26** (1987) 173.

44 P. Poganiuch, P. Gütlich, Inorg. Chem. **26** (1987) 455.

45 A. Hauser, J. Adler, P. Gütlich, Chem. Phys. Lett. **152** (1988) 468.

46 M. A. Hoselton, R. S. Drago, L. J. Wilson, N. Sutin, J. Amer. Chem. Soc. **98** (1976) 6967.

47 E. V. Dose, M. A. Hoselton, N. Sutin, M. F. Tweedle, L. J. Wilson, J. Amer. Chem. Soc. **100** (1978) 1141.

48 R. A. Bistead, J. K. Beattie, T. G. Dewey, D. H. Turner, J. Amer. Chem. Soc. **102** (1980) 6442.

49 J. J. McGarvey, I. Lawthers, J. Chem. Soc. Chem. Commun. 1982, 906.

50 J. DiBenedetto, V. Arkle, H. A. Goodwin, P. C. Ford, Inorg. Chem. **32** (1985) 456.

51 P. Adler, H. Spiering, P. Gütlich, J. Chem. Phys. Solids **50** (1988) 587.

52 P. Adler, A. Hauser, A. Vef, H. Spiering, P. Gütlich, Hyperfine Interactions **47** (1988) 343.

53 G. Ritter, E. König, W. Irler, H. A. Goodwin, Inorg. Chem. **17** (1988) 224.

54 H. A. Goodwin, K. H. Suggiyarto, Chem. Phys. Lett. **55** (1987) 11.

55 J. T. Hupp, M. J. Weaver, J. Phys. Chem. **89** (1985) 2795.

56 C.-L. Xie, D. N. Hendrickson, J. Amer. Chem. Soc. **109** (1987) 6981.

57 A. Hauser, to be published.

58 C. Hennen, R. Grimm, to be published.

59 E. Buhks, G. Navon, M. Bixon, J. Jortner, J. Amer. Chem. Soc. **102** (1980) 2918.